Acta Cryst. (1964). **17**, 827

The Short-Range Structure of Copper-16 At. % Aluminum

By Bernard Borie and C. J. Sparks, Jr.

Metals and Ceramics Division, Oak Ridge National Laboratory, Oak Ridge, Tennessee, U.S.A.*

(*Received* 15 *July* 1963)

The distribution of diffuse X-ray scattering in two planes in reciprocal space for the substitutional solid solution copper–16 at. % aluminum was measured. The symmetry of the distribution showed that there is not only short-range order but as well small static atomic displacements from the expected sites. The short-range order intensity was separated from that associated with the static displacements and the two were treated separately.

It was found that the order parameters were satisfactorily reproduced by the following model: The Al atoms are distributed on the atomic sites in sets of four so that they occupy the corners of a distorted tetrahedron. The tetrahedra are distributed at random except that no two may be so close that they form an Al–Al nearest neighbor pair. All other sites are occupied by Cu atoms.

Measurements after neutron irradiation showed that such exposure caused a small but significant increase in the state of order.

Introduction

The face-centered cubic substitutional solid solution, copper–16 at.% aluminum, became of interest because of the radiation damage experiments of Wechsler & Kernohan (1958, 1962) and Kernohan & Wechsler (1961). These experiments showed that the electrical resistivity of this alloy decreases as a function of time in the reactor, passes through a minimum, and then increases continuously. Since pure metals do not exhibit such a decrease, it was suggested that the resistivity change may be associated with a radiation-induced change in the short-range order present in the alloy. To determine whether or not this is the case, diffuse X-ray scattering measurements were made on single crystals of the alloy before and after exposure to reactor irradiation. Reported here are the results of those measurements and their interpretation.

As will be seen, an interesting and different distribution of diffuse intensity was found, reflecting not only short-range order but as well displacements of atoms from the sites of the average lattice. The combined interpretation of the short-range order diffuse scattering and the modulations resulting from the atomic displacement yields an unexpected short-range structure for copper–aluminum solid solutions.

Measurements of short-range order before and after irradiation for this alloy have been reported by Houska & Averbach (1959). However, their use of a powder sample results in an averaging of the intensity over a sphere about the origin in reciprocal space. This consequent loss of detail in the intensity distribution causes a precise interpretation of the observed order parameters to be very difficult.

* Operated for the U.S. Atomic Energy Commission by Union Carbide Corporation.

Experimental

A single crystal of intended composition copper–16 at.% aluminum was grown in a graphite mold and homogenized at 750 °C for 2 hr followed by slow cooling to room temperature at a rate of about 20 °C per hr. Slabs 5/8 in. in diameter of appropriate orientation were cut from the ingot and polished mechanically and electrolytically to remove the distorted surface layer and to produce a bright, clean surface. The samples were then annealed at 150 °C for 54 hr in order to increase the amount of order.

The lattice constant of our alloy was observed to be $3{\cdot}654_5$ Å. This value corresponds closely to the intended composition of Cu–16 at.% Al, according to the measurements of Bradley & Goldschmit (1939), Obinata & Wasserman (1933), Stirling & Raynor (1955), and Wechsler & Kernohan (1958), all of which agree well with each other.

The diffractometer used for the diffuse scattering measurements was a General Electric XRD 5 equipped with a goniostat. The diffractometer was modified to step scan automatically and print for preset time. A lithium fluoride monochromator, doubly bent as suggested by Warren (1954), and Cu $K\alpha$ radiation were used. The detector was a sodium iodide scintillation counter with pulse height discrimination. A balanced pair of nickel–cobalt filters were used to eliminate the half-wavelength component from the monochromator and the copper fluorescence this component excites in the sample. The specimen was supported in a liquid nitrogen cryostat, so that measurements could be made either at room temperature or at −195 °C. The volume surrounding the sample was evacuated, to provide thermal insulation for the low-temperature measurements and to eliminate air scattering. All measurements were converted to absolute units by

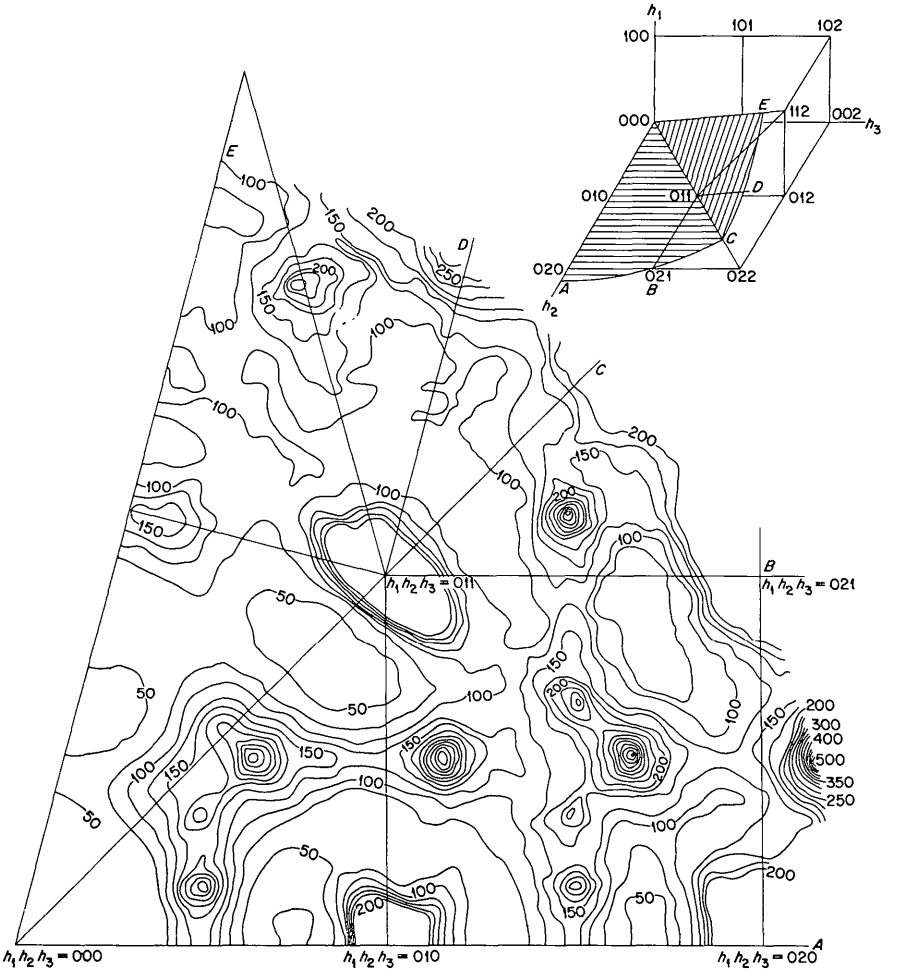

Fig. 1. The diffuse intensity distribution at −195 °C for the unirradiated sample. Compton scattering has been removed, but no temperature diffuse scattering correction has been made. The quantity plotted is $1000I$ (in electron units)/Nf^2_{Cu}. Closely spaced contours greater than 200 near the Bragg maxima have been omitted. The inset illustrates schematically the two planes in reciprocal space in which the measurements were made.

comparing the intensity with that observed at high scattering angles from an amorphous material, polystyrene.

Measurements at two temperatures were made in order to eliminate contributions to the diffuse scattering due to thermal motion. Since the temperature diffuse scattering is nearly proportional to the absolute temperature, a linear extrapolation to absolute zero was used.

The diffuse intensity was determined in two planes of reciprocal space: the h_1, h_2, 0 plane and the h_1, h_2, (h_1+h_2)plane. (h_1, h_2, and h_3 are continuous variables defining a point in reciprocal space.) The latter plane has hexagonal symmetry, with a [111] direction for its normal. Fig. 1 shows the diffuse intensity distribution in these two planes measured at −195 °C.

After completion of the diffuse intensity measurements, the samples were exposed for 157 hr at 100 °C in hole D at the center of the ORNL Graphite Reactor. The integrated thermal neutron flux for this exposure is approximately $5{\cdot}2 \times 10^{17}$ neutrons cm^{-2}. A resistivity sample of similar composition to the X-ray samples was irradiated in the same capsule. The exposure caused the resistivity to decrease from 8·472 to 8·335 μohm.cm. This decrease corresponds closely to the minimum in the resistivity *versus* time of irradiation for an irradiation temperature of 100 °C (Kernohan & Wechsler, 1961). Following the irradition, the diffuse scattering measurements were repeated. Figs. 2 and 3 compare the intensity distribution before and after irradiation for the two planes in reciprocal space.

It is clear from the figures that the effect of neutron irradiation is a slight sharpening of the pattern, corresponding to small increases in the magnitudes of the order parameters, but the general features of the intensity distribution are the same. This is substantially in agreement with the previously reported result of Houska & Averbach (1959).

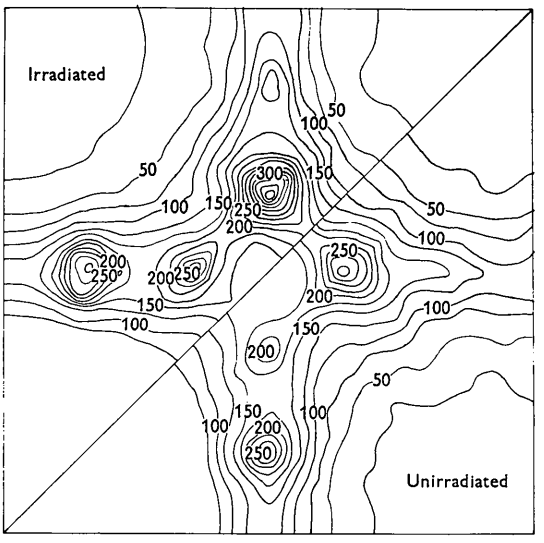

Fig. 2. A comparison of the diffuse intensity distribution in the (h_1h_20) plane for the irradiated and unirradiated samples. The intensity is shown in the square $0<h_1, h_2<1$. The quantity plotted is the same as in Fig. 1, except that the temperature diffuse scattering has been removed.

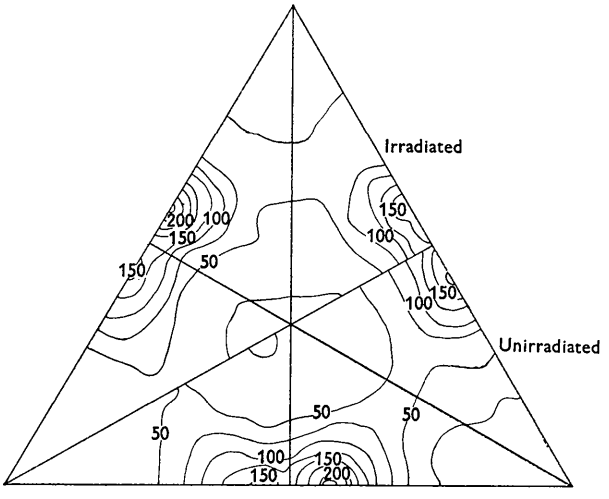

Fig. 3. A comparison of the diffuse intensity distribution in the (h_1, h_2, h_1+h_2) plane for the irradiated and unirradiated samples. The intensity is shown in the triangle $0<h_1+h_2<1$. The quantity plotted is the same as in Fig. 2.

Determination of the short-range structure parameters

The interpretation of the intensity patterns of Figs. 2 and 3 is most usefully done in terms of the size effect theory of Warren, Averbach & Roberts (1951). According to their result, for a face-centered cubic substance the diffuse intensity in electron units per atom (I/N), divided by $m_Am_B(f_A-f_B)^2$, may be written as the sum of two series:

$$I(h_1h_2h_3)/Nm_Am_B(f_A-f_B)^2 = \sum_{lmn}\alpha_{lmn}\cos 2\pi(h_1l+h_2m+h_3n) - \sum_{lmn}2\pi\beta_{lmn}(h_1l+h_2m+h_3n)\sin 2\pi(h_1l+h_2m+h_3n).$$

The sums are taken over all values of the integers l, m, and n. The two kinds of atom have scattering factors f_A and f_B, and their atomic concentrations in the alloy are m_A and m_B. The continuous variables h_1, h_2, and h_3 define a point in reciprocal space, and at the Bragg maxima they take on values equal to half of the Miller indices. The integers lmn define a particular lattice site

$$\mathbf{r}_{lmn} = l(\mathbf{a}_1/2)+m(\mathbf{a}_2/2)+n(\mathbf{a}_3/2)$$

where $\mathbf{a}_1\mathbf{a}_2\mathbf{a}_3$ are the cubic unit-cell vectors. For a face-centered cubic structure $l+m+n$ must be even. The short-range order parameter α_{lmn} and the size effect parameter β_{lmn} are as defined by Warren *et al.* (1951). All α_{lmn} except α_{000} vanish if the atoms are randomly distributed on the sites, and all β_{lmn} vanish if all of the atoms lie precisely on the sites of the average lattice.

Since our measurements were all of intensity distributions in planes of reciprocal space, it is useful to rewrite the intensity in its two-dimensional form:

$$I'(h_1h_2) = \sum_{pq} A_{pq}\cos 2\pi(h_1p+h_2q) - \sum_{pq}(h_1B^p_{pq}+h_2B^q_{pq}) \times \sin 2\pi(h_1p+h_2q)\,. \quad (1)$$

In the h_1h_20 plane

$$I' = \frac{Nm_Am_B(f_A-f_B)^2}{I(h_1h_20)},\ A_{pq} = \sum_n \alpha_{pqn},\ \text{and}\ B^p_{pq} = 2\pi p\sum_n \beta_{pqn}\,;$$

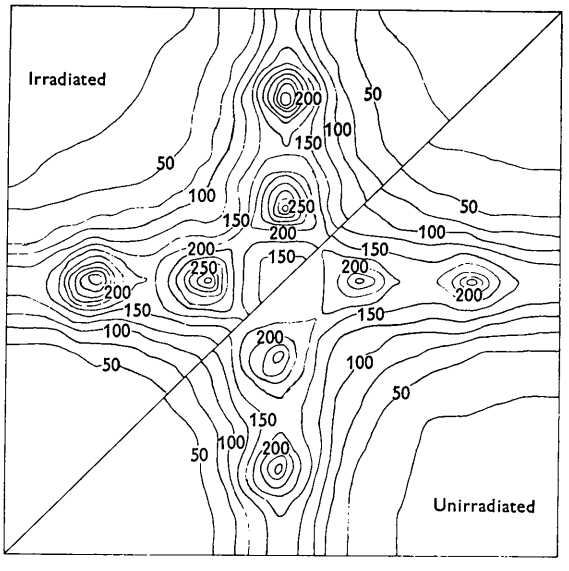

Fig. 4. The intensity distribution of Fig. 2 after removal of the atomic displacement modulations.

Table 1. *Observed and computed values of A_{pq}*

	$(h_1, h_2, 0)$ plane				(h_1, h_2, h_1+h_2) plane		
	Observed				Observed		
pq	Irrad.	Unirrad.	Calc.	pq	Irrad.	Unirrad.	Calc.
00	+1·886	+1·732	+1·500	00	+1·209	+1·354	+0·848
10	−0·669	−0·610	−0·564	10	−0·161	−0·139	−0·129
11	−0·024	−0·063	−0·072	21	−0·225	−0·205	−0·184
20	+0·252	+0·254	+0·231	20	+0·171	+0·177	+0·205
21	+0·099	+0·086	+0·100	31	−0·012	−0·015	−0·036
22	−0·124	−0·080	−0·172	30	+0·064	+0·053	+0·055
30	−0·195	−0·168	−0·156	42	+0·036	+0·034	+0·020
31	−0·026	−0·032	−0·077	41	−0·061	−0·063	−0·076
32	+0·050	+0·024	+0·044	40	+0·013	+0·008	−0·034
40	+0·060	+0·072	+0·074	52	+0·030	+0·020	+0·022
41	+0·089	+0·050	+0·028	51	−0·012	−0·012	−0·006
33	−0·009	+0·004	+0·030	50	+0·044	+0·034	+0·033
42	−0·074	−0·040	+0·004	63	−0·019	−0·017	+0·002
43	+0·038	+0·026	−0·002	62	+0·006	+0·003	+0·005
50	−0·064	−0·052	0·000	61	−0·012	−0·012	+0·010
51	−0·023	−0·024	−0·001	60	+0·001	−0·003	−0·001
52	+0·026	+0·018	+0·008	73	+0·003	0·000	+0·002
44	−0·077	−0·045	+0·016	72	+0·010	+0·012	+0·004
53	−0·008	−0·007	+0·011	71	−0·009	−0·007	+0·001
60	+0·076	+0·044	+0·005	84	−0·006	−0·001	+0·008
61	−0·018	−0·006	+0·004	70	+0·013	+0·011	+0·001
62	+0·020	+0·001	+0·001	83	−0·007	−0·005	+0·009
54	+0·041	+0·022	+0·004	82	−0·002	−0·002	+0·005
63	−0·027	−0·002	0·000	81	−0·004	−0·004	+0·002
70	−0·027	−0·011	0·000	94	+0·007	+0·003	+0·002
55	−0·017	−0·010	+0·002	93	−0·001	−0·001	+0·002
71	−0·018	−0·003	0·000	80	+0·004	0·000	0·000

and in the h_1, h_2, h_1+h_2 plane

$$I' = \frac{I(h_1, h_2, h_1+h_2)}{Nm_Am_B(f_A-f_B)^2}, A_{pq} = \sum_n \alpha_{p-n,\, q-n,\, n}, \text{ and}$$

$$B^p_{pq} = 2\pi p \sum_n \beta_{p-n,\, q-n,\, n}\,.$$

A method is available (Borie, 1961) to separate the two series of equation (1). Figs. 4 and 5 show the intensity distributions after removal of the atomic size effect modulations. Fourier inversion of these plots, done with the aid of an IBM 7090, yielded the parameters A_{pq}, which are given in Table 1. Table 2 gives B^p_{pq} for the unirradiated sample in the h_1h_20 plane.

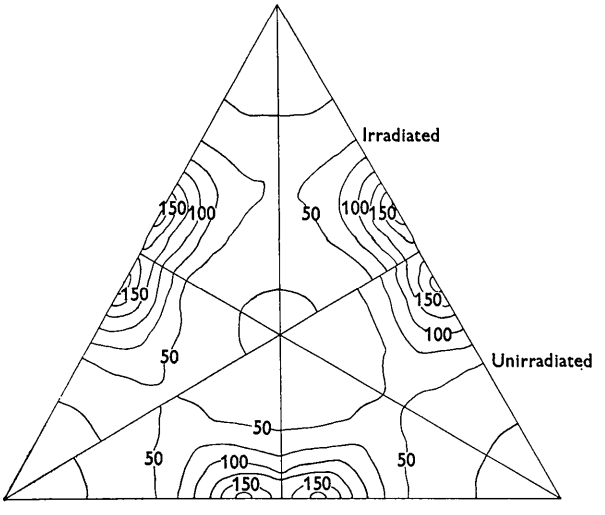

Fig. 5. The intensity distribution of Fig. 3 after removal of the atomic displacement modulations.

Table 2. *Observed values of B^p_{pq} for the unirradiated sample in the (h_1h_20) plane*

	$p = 1$	2	3	4	5
$q = 0$	−0·019	−0·104	+0·006	+0·028	−0·005
1	−0·031	+0·147	−0·023	−0·022	−0·004
2	+0·002	−0·101	+0·004	+0·034	−0·021
3	+0·016	+0·058	+0·002	−0·021	+0·017
4	−0·019	−0·026	−0·009	+0·015	−0·012

Interpretation of the parameters A_{pq}

We defer to a later section a discussion of the effect of radiation, and consider first the rather more interesting problem of interpreting the diffuse scattering in terms of the short-range structure of the alloy.

The parameters A_{pq} define the diffuse scattering which would have been observed if none of the atoms were displaced from the sites of the average lattice. The diffuse peaks shown in Figs. 4 and 5 do not occur at the normal superstructure positions, but rather, they form a 'four-leaf clover' arrangement of satellites about each superstructure position, in a fashion similar to that found by Guinier & Griffoul (1948) for Cu_3Au quenched from high temperature and then heat treated for a short time below the critical temperature. They

interpreted their pattern in terms of highly ordered antiphase domains, the domains being bounded by faults on the (100) planes in such a way that gold atoms have only copper nearest neighbors. As the domain size increases, the satellites become closer to the normal superstructure positions, finally merging with each other at these points as the domains become large.

In our case, the satellites are quite a bit further from the superstructure positions than those found by Guinier & Griffoul. In fact, the intensity seems to cluster about points half-way between them and to be relatively weak at points such as $h_1h_20=\frac{1}{2}\frac{1}{2}0$. This would imply an extremely small domain size.

The above considerations make it tempting to assume that the atomic configuration at a domain boundary is the most common atomic arrangement in our alloy. Fig. 6 illustrates how the crossing of such a boundary (the xy plane) gives rise to distorted tetrahedral arrays.

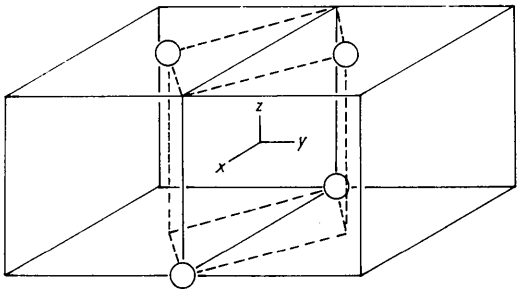

Fig. 6. Two face-centered cubic unit cells shown schematically to illustrate the atomic sites of the distorted tetrahedron discussed in the text.

In principle, one should be able to obtain a set of α_{lmn} from a least-squares fit to the experimentally determined A_{pq} in two planes in reciprocal space. In practice it was found that the α_{lmn} were overdetermined and a variety of results could be obtained depending on how the various equations in α_{lmn} are weighted relative to each other. However, all sets of α_{lmn} so determined which are reasonably plausible include a value of α_{110} of about $-0{\cdot}2$, the largest possible negative value this parameter may take on. This means that there are no Al–Al nearest neighbors in the alloy. This is consistent with the tetrehedral arrangement of Fig. 6 if the corner atoms are taken to be Al and if all of the nearest neighbors of the four corner positions are taken to be Cu.

There is a further factor which tends to make the existence of such tetrahedra plausible. The measurements of Bradley & Goldschmit (1939), Obinata & Wasserman (1933), and Stirling & Raynor (1955) all show the atomic volume to increase much more slowly with increasing Al content than one would compute from the lattice constants of pure Cu and pure Al. If one extrapolates to 25 at.% Al, one obtains just the average atomic volume found by Tarora (1949) for β_1 Cu_3Al. This phase is metastable and results upon quenching the β phase (b.c.c., disordered) to room temperature. Furthermore, the β_1 phase has the $BiF_3(DO_3)$ structure, in which regular tetrahedra are delineated by the Al atoms occupying four of the eight corners of a body-centered cell. In this structure there are no Al–Al nearest neighbors. The dotted cell of Fig. 6 shows such a tetrahedron, distorted to fit a face-centered cubic lattice.

In the light of the above, it was decided to attempt to compute α_{lmn} from the following model: The alloy is composed of Al tetrahedra as shown in Fig. 6. They are distributed more or less at random on the sites of a lattice otherwise populated by copper atoms, with the restriction that no two tetrahedra may be so near each other that they cause Al–Al nearest neighbors. There are six possible orientations of tetrahedra, all assumed to be equally probable. One orientation is shown in Fig. 6; a second orientation may be obtained by a 90° rotation about the z axis. In Fig. 6 the extended axis is along the z axis; the four other orientations are obtained by allowing the extended axis of the tetrahedron to be parallel to the other two cube axes.

To compute the diffuse intensity for this model it is convenient to rearrange the intensity expression. The short range order parameter α_t associated with the lattice vector $\mathbf{r}_t$ may be written $\alpha_t=1-(p^t_{BA}/m_B)$. The quantity p^t_{BA} is the probability of finding a B atom at site t after first having found an A atom at the origin. With $p^t_{BA}=1-p^t_{AA}$, since $m_B=1-m_A$, we may write $\alpha_t=1-(1-p^t_{AA})/m_B=p^t_{AA}/m_B-m_A/m_B$. With $f_A-f_B=\Delta f$ we may write I_{SRO}, the intensity associated with short range order, in electron units (Cowley, 1950)

$$I_{SRO}/\Delta f^2 = Nm_Am_B\sum_t \alpha_t \exp(i\mathbf{k}\cdot\mathbf{r}_t)$$
$$= \sum_t Nm_Ap^t_{AA}\exp(i\mathbf{k}\cdot\mathbf{r}_t) - \sum_t Nm_A^2\exp(i\mathbf{k}\cdot\mathbf{r}_t).$$

The quantity $Nm_Ap^t_{AA}$ in the first sum J is simply the total number of $A-A$ pairs in the crystal separated by $\mathbf{r}_t$. In the second J_R, Nm_A^2 is the number of pairs that would have been obtained if the atoms were distributed at random. Hence the problem of computing I_{SRO} from a model rests in a calculation of J. If φ is an amplitude such that $J=\varphi\varphi^*$, then $\varphi=\sum_A \exp(i\mathbf{k}\cdot\mathbf{r}_t)$. The summation for φ is taken only over those sites occupied by A atoms.

We wish to write φ in terms of the tetrahedra, and to do that it is convenient to assign to each tetrahedron a structure factor. With the origin chosen to be the center of the tetrahedron, for the orientation shown in Fig. 6 we may write

$$F = \exp[2\pi i(h_1-h_3)]+\exp[2\pi i(-h_1-h_3)] + \exp[2\pi i(h_2+h_3)]+\exp[2\pi i(-h_2+h_3)].$$

Similar structure factors may be written for the other five orientations. Then $\varphi=\sum F_t\exp(i\mathbf{k}\cdot\mathbf{r}_t)$. The summation is now carried out only over those sites which

are centers of tetrahedra. This is one-fourth of the total number of Al sites. If site t is the center of a tetrahedron, F_t may be any one of six possible structure factors. We may then write

$$J = \sum_t \sum_{t'} F_t F_{t'}^* \exp\left[i\mathbf{k}.(\mathbf{r}_t - \mathbf{r}_{t'})\right].$$

Let p_{lmn} be the probability of finding a tetrahedron at $\mathbf{r}_{lmn}$ after first having found one at the origin. Then

$$J = (Nm_A/4) \sum_{lmn} p_{lmn} \langle FF^* \rangle_{lmn} \exp\left[2\pi i(h_1 l + h_2 m + h_{3n})\right].$$

To compute $\langle FF^* \rangle_{lmn}$, we assume that if several relative orientations of the two tetrahedra are possible, they are all equally probable. For J_R, $p_{lmn} = m_A/4$ and $\langle FF^* \rangle_{lmn} = \langle F \rangle^2$. So

$$I_{SRO}/\Delta f^2 = (Nm_A/4) \sum_{lmn} \{p_{lmn} \langle FF^* \rangle_{lmn} - (m_A/4)\langle F \rangle^2\} \exp\left[2\pi i(h_1 l + h_2 m + h_3 n)\right].$$

It is straightforward but tedious to compute from the above expression the probability of finding Al–Al pairs in the various coordination shells and hence the α_{lmn}, once p_{lmn} is given. Reasonable values for p_{lmn} were assumed in the following way: For r_{lmn} greater than some $\mathbf{r}_{LMN}$, $p_{lmn} = m_A/4$, $\langle FF^* \rangle_{lmn} = \langle F \rangle^2$, and there is no contribution to I_{SRO} associated with that coordination shell. To conserve the composition of the alloy, the average value of p_{lmn} within the sphere of radius $\mathbf{r}_{LMN}$ must be $m_A/4$. Given a tetrahedron at the origin ($p_{000} = 1$), p_{lmn} for the first several coordination shells must be zero in order to avoid creating Al–Al nearest neighbors. Specifically, $p_{lmn} = 0$ for $lmn = 110$, 200, and 211. The first possible tetrahedron sites are in the 220 shell, and only a few of the six possible orientations are allowed. The largest $\mathbf{r}_{lmn}$ for which fewer than all six tetrahedral orientations are possible is $lmn = 330$. Hence, there should be short-range order among the tetrahedra at least out to that shell. We assumed that $L^2 + M^2 + N^2 = 20$, which should correspond to the minimum amount of order possible, given that all the Al atoms are arranged in tetrahedra. For $6 < l^2 + m^2 + n^2 < 20$, p_{lmn} must be greater than $m_A/4$ in order to compensate for the forbidden sites near the origin. Presumably it must begin at $lmn = 220$ with a moderately large value and decrease slowly to $m_A/4$ at $lmn = 420$. In the range $6 < l^2 + m^2 + n^2 < 20$, the probability was taken to be $p_{lmn} = m_A/4 + K/(20 - l^2 - m^2 - n^2)$, the constant K being chosen to conserve the composition of the alloy within the sphere of radius r_{420}. Table 3 gives the short-range order parameters computed with this model.

Table 3. *Calculated three-dimensional short-range order parameters from the tetrahedron model*

lmn	α_{lmn}	lmn	α_{lmn}
000	+1·000	431	0·000
110	−0·190	521	+0·002
200	+0·213	440	+0·008
211	+0·045	530	+0·007
220	−0·004	433	−0·001
310	−0·083	442	+0·004
222	−0·076	600	+0·003
321	+0·003	611	+0·002
400	+0·034	532	+0·002
411	+0·012	620	+0·001
330	−0·002	541	+0·002
420	+0·012	622	0·000
332	+0·017	631	0·000
422	−0·008	444	0·000
510	−0·009	550	+0·002

Table 1 compares the observed values of A_{pq} with those computed from tha above model. A more complicated model, allowing certain relative orientations of the tetrahedra to be preferred, could probably improve the agreement. However, it was felt that the agreement obtained was sufficiently good not to make this elaboration worthwhile.

Interpretation of the parameters B_{pq}^p

It is evident from the figures that the modulations of the diffuse intensity associated with the series in B_{pq}^p (equation 1) are both large and unusual. A comparison of Figs. 2 and 3 with 4 and 5 shows that a considerable difference in the intensity distribution results when they are removed. In other systems in which the effect has been observed (Roberts, 1954; Batterman, 1957; Borie, 1957), it is found that the short-range order diffuse intensity is distorted most by their presence along lines in reciprocal space through the fundamental reflections such as $h_1 00$ or $h_1 10$. In this alloy, however, as may be seen from Fig. 1, the effect of the modulations is most apparent along lines such as $h_1 \frac{1}{2} 0$ or $h_1 \frac{3}{2} 0$; that is to say, along lines through the usual superstructure positions for a face-centered cubic alloy.

In general one would expect that all β_{lmn} would have a common sign — a consequence of the fact that the distance between pairs of 'larger' atoms for all combination shells is greater than the distance computed from the average undistorted lattice. Table 2 shows that for this alloy both positive and negative values of β_{lmn} occur. This means that for some coordination shells the distance between say Al–Al pairs is greater than that associated with the average lattice, and for some others is is less.

It is also frequently supposed that the largest β_{lmn} is associated with the first coordination shell, and that β_{lmn} becomes smaller as $l^2 + m^2 + n^2$ becomes larger. Table 2 shows that for this alloy this is not so. The largest value of B_{pq}^p occurs for $pq = 21$, which is independent of both the first and second coordination shells. The next largest value (for $pq = 20$) is of opposite sign and independent also of the nearest neighbors. In fact, those B_{pq}^p which are influenced by the nearest neighbors ($pq = 10$ and 11) are quite small compared with at least three other B_{pq}^p.

The data of Table 2 show another interesting anomaly which may not be explained in terms of the

simple size effect theory as developed by Warren, Averbach & Roberts (1951). For the lmn coordination shell, let $\mathbf{R}_{lmn}^{AA}$ be the average vector separation between pairs of A atoms, and let $\mathbf{r}_{lmn}$ be the vector separation that would have been found if there were no static displacements from the sites of the average lattice. Then

$$\mathbf{R}_{lmn}^{AA} = \mathbf{r}_{lmn} + \boldsymbol{\delta}_{lmn}^{AA} .$$

In the Warren–Averbach–Roberts theory it was assumed that this relation could be written

$$\mathbf{R}_{lmn}^{AA} = \mathbf{r}_{lmn}(1+\varepsilon_{lmn}^{AA}) \tag{2}$$

where ε_{lmn}^{AA} is a small scalar. That is, it was assumed that $\boldsymbol{\delta}_{lmn}^{AA}$ is always parallel to $\mathbf{r}_{lmn}$. A consequence of this assumption is that the theory can be developed in terms of a set of parameters β_{lmn} which are determined by ε_{lmn}^{AA}, ε_{lmn}^{BB}, and α_{lmn}. β_{lmn} is independent of the order of l, m, and n and is thus a constant for any coordination shell. In the h_1h_20 plane, since $B_{pq}^p = 2\pi p \sum_n \beta_{pqn}$, it follows that $(1/p)B_{pq}^p = (1/q)B_{pq}^p$. Table 2 shows quite clearly that the data do not have this property. For example $\frac{1}{2}B_{21}^2 = \frac{1}{2}(+0{\cdot}147) = 0{\cdot}073$, while $B_{12}^1 = +0{\cdot}002$, a difference which is quite outside the accuracy of the measurements. A similar comparison may be made between B_{31}^3 and B_{13}^1, and between B_{32}^3 and B_{23}^2. Hence, for this alloy, the assumption that $\boldsymbol{\delta}_{lmn}^{AA} = \mathbf{r}_{lmn}\varepsilon_{lmn}^{AA}$ does not hold, and the diffraction theory must be modified. That this might be so in some cases has been suggested by Guinier (1954).

The Warren–Averbach–Roberts treatment may be easily modified to obtain a more general expression valid for this alloy. With

$$\boldsymbol{\delta}_{lmn}^{AA} = L_{lmn}^{AA}\tfrac{1}{2}\mathbf{a}_1 + M_{lmn}^{AA}\tfrac{1}{2}\mathbf{a}_2 + N_{lmn}^{AA}\tfrac{1}{2}\mathbf{a}_3$$

and

$$\boldsymbol{\delta}_{lmn}^{BB} = L_{lmn}^{BB}\tfrac{1}{2}\mathbf{a}_1 + M_{lmn}^{BB}\tfrac{1}{2}\mathbf{a}_2 + N_{lmn}^{BB}\tfrac{1}{2}\mathbf{a}_3$$

one finds that I_{AD}, the contribution to the diffuse intensity associated with the atomic displacements, may be written in electron units

$$\begin{aligned} I_{AD}/Nm_Am_B(f_A-f_B)^2 &= -2\pi/(f_A-f_B)\sum_{lmn}[h_1\{L_{lmn}^{AA}(\alpha_{lmn}+(m_A/m_B))f_A \\ &\qquad -L_{lmn}^{BB}(\alpha_{lmn}+(m_B/m_A))f_B\} \\ &\quad +h_2\{M_{lmn}^{AA}(\alpha_{lmn}+(m_A/m_B))f_A \\ &\qquad -M_{lmn}^{BB}(\alpha_{lmn}+(m_B/m_A))f_B\} \\ &\quad +h_3\{N_{lmn}^{AA}(\alpha_{mn}+(m_A/m_B))f_A \\ &\qquad -N_{lmn}^{BB}(\alpha_{lmn}+(m_B/m_A))f_B\}] \\ &\quad \times \sin 2\pi(h_1l+h_2m+h_3n) . \end{aligned} \tag{3}$$

Except that the assumption of equation (2) has not been made, the derivation is exactly parallel to that of Warren, Averbach & Roberts. If we let

$$\begin{aligned} \gamma_{lmn}^l = (2\pi/f_A-f_B)\{&L_{lmn}^{AA}(\alpha_{lmn}+(m_A/m_B))f_A \\ &-L_{lmn}^{BB}(\alpha_{lmn}+(m_B/m_A))f_B\} \end{aligned} \tag{4}$$

with similar expressions for γ_{lmn}^m and γ_{lmn}^n, equation (3) becomes

$$\begin{aligned} I_{AD}/Nm_Am_B(f_A-f_B)^2 = -\sum_{lmn}&(h_1\gamma_{lmn}^l+h_2\gamma_{lmn}^m+h_3\gamma_{lmn}^n) \\ &\times \sin 2\pi(h_1l+h_2m+h_3n) . \end{aligned} \tag{5}$$

We may imagine the γ's to be components of an atomic displacement vector $\boldsymbol{\Gamma}_{lmn} = (\gamma_{lmn}^l, \gamma_{lmn}^m, \gamma_{lmn}^n)$ of arbitrary magnitude and direction. With the assumption of equation (2), it becomes $\boldsymbol{\Gamma}_{lmn} = 2\pi\beta_{lmn}(l, m, n)$, and equation (5) reduces to the Warren–Averbach–Roberts result. For highly symmetrical values of lmn such as 110 or 200, this is an adequate representation of $\boldsymbol{\Gamma}_{lmn}$. But for say $lmn = 211$, there is no physical necessity that $\gamma_{211}^2 = 2\gamma_{211}^1$.

In the h_1h_20 plane, then, with I_{AD} given by (5), we may write

$$B_{pq}^p = \sum_n \gamma_{pqn}^p . \tag{6}$$

We will not attempt the very difficult task of finding a model which will reproduce all B_{pq}^p. Rather, we will compute only the first several using the basic tetrahedron arrangement applied to the short-range order coefficients. We will show that if one displaces the four aluminum atoms which make up the tetrahedron from their sites in such a way that the tetrahedron becomes more regular, one obtains reasonably good agreement with the experimentally observed values.

Consider the dashed body-centered cell of Fig. 6, with aluminum atoms at four of its eight corners forming a tetrahedron. Let the aluminum atoms be moved from their sites so that the dotted cell is cubic and the tetrahedron is undistorted. If this is done so that the atomic volume within the dotted cell is the same as that of the undistorted f.c.c. cell, then the dotted cell edge a is related to the f.c.c. lattice constant a_0 by $\frac{1}{2}a^3 = \frac{1}{4}a_0^3$, or $a = 0{\cdot}8a_0$. With aluminum atoms labeled A, we have that

$$\boldsymbol{\delta}_{200}^{AA} = \sqrt{2}(0{\cdot}8\,a_0) - a_0 = 0{\cdot}13\,a_0 \text{ or } \boldsymbol{\delta}_{200}^{AA} = (+0{\cdot}26\tfrac{1}{2}a_0, 0, 0).$$

Similarly

$$\boldsymbol{\delta}_{211}^{AA} = (-0{\cdot}40\tfrac{1}{2}a_0,\ +0{\cdot}13\tfrac{1}{2}a_0,\ +0{\cdot}13\tfrac{1}{2}a_0) .$$

We have ignored all contributions to $\boldsymbol{\delta}_{lmn}^{AA}$ except those associated with a single tetrahedron.

There are no AA nearest neighbor pairs so that $\boldsymbol{\delta}_{110}^{AA}$ is meaningless. However, for the copper atom occupying the body-centered position of the dotted cell, $\boldsymbol{\delta}_{110}^{AB} = 0$, since the atomic volume of the tetrahedron is unchanged by the atomic displacements.

If we ignore the contribution of BB pairs to equation (4) on the grounds that they should not be significantly affected by a distortion conserving atomic volume, and if we take f_A and f_B to be proportional to the atomic numbers of aluminum and copper, we have

$$\gamma_{lmn}^l = -2\pi(\tfrac{13}{16})(\alpha_{lmn}+(m_A/m_B))L_{lmn}^{AA} .$$

Since only one of the six 200 neighbors can be a part of the tetrahedron (see Fig. 6) we take

$$\alpha_{200} = 1-(\tfrac{5}{6}/0{\cdot}84) = +0{\cdot}01\ ,$$

and

$$\gamma^2_{200} = -2\pi(\tfrac{13}{16})(0{\cdot}01+0{\cdot}19)(+0{\cdot}26) = -0{\cdot}27\ .$$

Similarly

$$\gamma^2_{211} = +0{\cdot}20 \text{ and } \gamma^1_{211} = -0{\cdot}07\ .$$

The above calculation was made assuming that the atomic displacements were such that the tetrahedron is regular. If the displacements are only one-third *that great*, and if we use equation (6) to compute B^p_{pq}, we find that $B^1_{10}=0{\cdot}000$, $B^1_{11}=-0{\cdot}047$, $B^1_{12}=-0{\cdot}047$, $B^2_{20}=-0{\cdot}090$, and $B^2_{21}=+0{\cdot}133$. These values agree quite well with those given in Table 2, except for B^1_{12} which is in any case small and could easily be influenced by the higher order γ^l_{lmn} contributions which have been omitted. The two largest values of B^p_{pq} of Table 2 have been reasonably well reproduced by the calculation.

This interpretation of the atomic displacement effect in this alloy is admittedly crude, and necessarily dependent on assumptions which, though plausible, are hardly certain. It does, however, seem to confirm that the tetrahedra are more nearly regular than one would compute from the average lattice constant.

Discussion

It has been shown from an interpretation of diffuse scattering measurements that the short-range structure of the alloy copper–16 at.% aluminum consists of a more or less random arrangement of tetrahedra of aluminum atoms. The four corners of the tetrahedron are occupied by aluminum atoms, and its center is a copper site. All of the nearest neighbors of the four corner sites are copper so that there are no Al–Al pairs in the first coordination shell. Of the six tetrahedron edges, two are second-nearest neighbor distances and four are third-nearest neighbor distances, so that the tetrahedron is not regular. However, the atomic displacement modulations of the diffuse scattering show that the aluminum atoms are displaced from the sites of the average lattice in such a way that the tetrahedra become more nearly regular.

It is clear that the unusual atomic displacement modulations encountered in these measurements are not simply the consequence of atomic size as originally proposed by Warren, Averbach & Roberts (1951) and Guinier (1954), and as found in copper–gold alloys by Roberts (1954), Batterman (1957), and Borie (1957). They are rather the result of an effort to maintain the bond angles and distances of a regular tetrahedron, and they therefore show that the atomic bonds in this alloy have considerable non-metallic character. It is proposed that the atomic size effect originally treated by Warren, Averbach & Roberts be more generally called the atomic displacement effect.

Values of the experimentally determined B^p_{pq} in the $(h_1h_2h_0)$ plane are given for the unirradiated sample only because their interpretation is at the moment rather primitive, and because they are less accurately known than the A_{pq}. Essentially, their determination depends on a small difference between two numbers, while A_{pq} depends on the average (Borie, 1961). For the unirradiated sample, slightly larger B^p_{pq} were observed. The writers are convinced, however, that in principle much important information about the structure of disordered solid solutions is inherent in these parameters, and that much remains to be done both in terms of their measurement and their interpretation.

This experiment confirms the result of Houska & Averbach (1959) that the state of order has increased after irradiation, presumably because of radiation enhanced diffusion. However, Table 1 shows that the increases in the order parameters are small compared with those reported by Houska & Averbach, and in some cases A_{pq} is either unchanged or slightly decreased. In general the calculated A_{pq} seem to agree better with those measured with an unirradiated sample, though the difference is usually small. An analysis of the meaning of the changes in A_{pq} upon irradiation was not attempted. Note that radiation caused A_{00} to increase in the (h_1h_20) plane while it decreased in the (h_1,h_2,h_1+h_2) plane. However, the sum of A_{00} in the two planes is unchanged. This is consistent with the requirement that the average short-range order intensity is a constant and independent of the state of order. The rather large discrepancy between observed and calculated A_{00} in both planes is almost surely due to residual temperature diffuse scattering which the extrapolation failed to remove from the measurements. It should have little effect on other A_{pq}.

No effect of thermal motion on the sharpness of the diffuse scattering distribution was observed. This effect, originally proposed by Muldawer (1952) and more recently treated by Walker & Keating (1961) requires that as the temperature is raised the short-range order peaks become broader. Complications associated with this effect were intentionally avoided by making measurements as near to the origin in reciprocal space as possible, and by making all measurements at room temperature or below.

Very little if any of the intense diffuse scattering near the fundamental Bragg maxima for disordered alloys predicted by Huang (1947) and found by Borie (1957) for Cu_3Au was observed. In fact, after the extrapolation to eliminate the temperature diffuse scattering, the residual diffuse scattering near the Bragg maxima was quite flat and very weak. In view of the unusual character of the atomic displacements in this case, it is perhaps not surprising that the predictions of Huang's elastic model do not hold.

Though the model used here for comparison with experiment presumed that all of the aluminum atoms occur in sets of four to form tetrahedra, the quality of

the agreement with experiment is not so good that it precludes the possibility of occasional incomplete tetrahedra or occasional isolated aluminum atoms. It would be of considerable interest to study more dilute alloys to see whether the tetrahedral arrangement found here persists even when the concentration is so low that each aluminum atom has the chance to isolate itself completely from like second and third nearest neighbors. It is clear that the experimental techniques for measurements of the sort described here are now sufficiently refined that meaningful results for alloys considerably more dilute may be obtained.

The authors wish to thank M. S. Wechsler and R. H. Kernohan, who suggested the problem, prepared the samples, and carried out the irradiation.

References

BATTERMAN, B. W. (1957). *J. Appl. Phys.* **28**, 556.
BORIE, B. (1957). *Acta Cryst.* **10**, 89.
BORIE, B. (1961). *Acta Cryst.* **14**, 472.
BRADLEY, A. J. & GOLDSCHMIT, H. J. (1939). *J. Inst. Met.* **65**, 389.
COWLEY, J. M. (1950). *J. Appl. Phys.* **21**, 24.
GUINIER, A. & GRIFFOUL, R. (1948). *Acta Cryst.* **1**, 188.
GUINIER, A. (1954). *Bull. Soc. Franç. Minér. Crist.* **77**, 680.
HOUSKA, C. R. & AVERBACH, B. L. (1959). *J. Appl. Phys.* **30**, 525.
HUANG, K. (1947). *Proc. Roy. Soc.* A, **190**, 102.
KERNOHAN, R. H. & WECHSLER, M. S. (1961). *Phys. Chem. Solids*, **18**, 175.
MULDAWER, L. (1952). Private Communication.
OBINATA, I. & WASSERMAN, G. (1933). *Naturwissenschaften*, **21**, 382.
ROBERTS, B. W. (1954). *Acta Metallurg.* **6**, 172.
STIRLING, P. H. & RAYNOR, G. V. (1955). *J. Inst. Met.* **84**, 57.
TARORA, I. (1949). *Nippon Kinz. Gakk.* **13**, 1.
WALKER, C. B. & KEATING, D. T. (1961). *Acta Cryst.* **14**, 1170.
WARREN, B. E., AVERBACH, B. L. & ROBERTS, B. W. (1951). *J. Appl. Phys.* **22**, 1493.
WARREN, B. E. (1954). *J. Appl. Phys.* **25**, 814.
WECHSLER, M. S. & KERNOHAN, R. H. (1958). *Phys. Chem. Solids*, **7**, 307.
WECHSLER, M. S. & KERNOHAN, R. H. (1962). *Radiation Damage in Solids*, Vol. II, p. 81. Vienna: International Atomic Energy Agency.

Acta Cryst. (1964). **17**, 835

An Application of the Symbolic Addition Method to the Structure of L-Arginine Dihydrate

BY ISABELLA L. KARLE AND J. KARLE

U.S. Naval Research Laboratory, Washington 25, *D.C., U.S.A.*

(*Received* 25 *July* 1963)

The crystal structure of L-arginine dihydrate was determined directly by means of the symbolic addition phase determination procedure, using the complete three-dimensional data obtained from Cu radiation. The space group is $P2_12_12_1$ and the cell dimensions are:

$$a = 5{\cdot}68,\ b = 11{\cdot}87,\ \text{and}\ c = 15{\cdot}74\ \text{Å}\ .$$

The arginine molecule is a zwitterion with the guanidyl group, rather than the amino group, accepting an extra proton. Two planes characterize the arginine molecule, one through the acid group, and the other through the extended side chain which contains the guanidyl group. The dihedral angle between these planes is 74°. The arginine molecules and the water molecules each make infinite chains perpendicular to each other by hydrogen bonding. All 18 hydrogen atoms have been located.

Introduction

L-Arginine, $^{+}(H_2N)_2CNH(CH_2)_3CH(NH_2)COO^{-}$, is one of the amino acids essential for animal growth. It is also the most basic of the amino acids since, in addition to the α-amino group, it also contains a terminal guanidyl group. This investigation afforded a good opportunity to study a biologically important amino acid structure and its associated hydrogen bonding. It also provided a valuable experience in the first application of the symbolic addition method for phase determination (Karle & Karle, to be published) to a non-centrosymmetric crystal.

Experimental

Purified L-arginine was obtained from the Central Research Laboratories of General Mills, Inc. Recrystallization from water at room temperature yielded crystals of the dihydrate which were colorless, transpa-